DRUG DEVELOPMENT AND INDUSTRIAL PHARMACY, 13(15), 2667-2686 (1987)

HINDERED SETTLING IN UNFLOCCULATED SUSPENSIONS

Kailash C. Dhupar* and Eugene L. Parrott
Division of Pharmaceutics, College of Pharmacy
University of Iowa, Iowa City, Iowa 52242

ABSTRACT

The hindered settling of three sizes of microcapsules suspended at four different concentrations in silicone fluids with four viscosities was determined at 25°C in suspensions.

The viscosities of the various suspensions determined by a Stormer Viscometer indicated pseudoplastic behavior. A viscosity constant was calculated using the power law of the form:

$$\eta_s{}^N = \eta_k G$$

The sedimentation rate of suspensions of microcapsules was determined at low Reynolds numbers. An equation

$$V_s = [(\rho_s - \rho)g/18\eta] \cdot f(d, C, \eta_k)$$

was proposed in which the exponent of $[(\rho_s - \rho)g/18\ \eta]$ was shown to be one. Various sedimentation parameters were fitted by multiple linear regression method to a curve. The empirical equation obtained was:

$$V_s = [(\rho_s - \rho)g/18\ \eta]\ d^{1.63}\ (1/C^{1.27})\ \eta_k{}^{0.07}\ e^{-4.31}$$

A comparison of sedimentation rate against suspension concentra-

---

* Present address: Pharmaceutical R & D, Hoffmann-La Roche Inc., Nutley, N.J. 07110.

tion was made for values calculated from the classical Stokes equation, experimental values, and predicted values from the fitted equation.

INTRODUCTION

A pharmaceutical suspension is an important pediatric dosage form in which the dispersed phase may be from 0.5 to 40 percent. In evaluating the physical stability of a suspension, the hindered sedimentation of the suspended particles is important as many pharmaceutical suspensions have a high concentration of solid particles.

THEORY

The first important theoretical study of the forces acting on an immersed body moving relative to a viscous fluid was made in 1851 by Stokes (1). His derivation for the terminal falling velocity, V_o, of a single spherical particle in an infinite fluid equated the viscous drag and the effective gravitational force

$$3dV_o\pi\eta = \frac{\pi d^3}{6}(\rho_s - \rho)g \qquad \text{(Eq.1)}$$

and solving for V_o

$$V_o = \frac{d^2(\rho_s - \rho)g}{18\eta} \qquad \text{(Eq.2)}$$

where η is viscosity of fluid (Poise = gm/cm sec), V_o is velocity of sphere relative to fluid (cm/sec), d is diameter of spherical particle (cm), ρ_s is density of the spherical particle (gm/cm^3), ρ is density of the fluid (gm/cm^3), and g is acceleration due to gravity.

The above relation considers only a single particle flowing in an infinite fluid with the size of the particle being much larger than the mean free path of the fluid. However, as the particle becomes very small (i.e., approaches the mean free path of the fluid), the particle may slip by the fluid molecule unscathed on particle-fluid molecule collisions, and the resistance to motion is decreased. In other words Brownian motion effects the sedimentation to a large extent. The lower limit of particle size (2,3) for gravitational sedimentation is 1 to 3 microns. If the fluid is not infinite, the effects of the wall tend to decrease the rate of sedimentation, and the correction factors for wall effects are available in the literature (4).

In a slurry or suspension the influence of other particles on the system should be considered. The viscosity of the suspension is considerably higher than that of the pure fluid due to the interaction of the adsorbed boundary layer with those of the neighboring particles.

It would be desirable to have a correlation that would allow the calculation of hindered settling rates, V_S, in unflocculated suspensions based only on the physical properties of the solid and liquid, i.e.,

$$V_S = \frac{d^2(\rho_S - \rho)g}{18\eta} C_H \qquad \text{(Eq. 3)}$$

where C_H is the correction for hindered settling.

As the concentration of the suspension is increased, the observed settling rate falls below V_O, and at some minimum concentration a fundamental change occurs in the appearance of the sedimenting material. At less than this concentration, the suspension exhibits a general cloudiness with the opacity increasing with increasing depth from the surface, during the greater part of the settling time. At and greater than this concentration, an identifiable suspension-supernatant interface

forms early in the sedimentation time; this phenomenon is named hindered settling or batch sedimentation. During hindered settling, statistically no particle is likely to fall unhindered from its initial position to its point of rest irrespective of the particle size. When a suspension of high concentration settles, the suspension-supernatant interface falls while the sediment interface rises from the bottom of the settling chamber.

Hindered settling of unflocculated particles in a fluid occurs when there is an interaction between particles. Although the laws of free settling, which seldom occurs in industrial practice, have been thoroughly studied, the quantitative expression of the settling velocity of particles in hindered settling conditions is still to be determined.

The hindered settling conditions differ from the free settling conditions in three aspects (5). With hindered settling, there is an equal volume of displaced liquid flowing upwards as the solid settles. Also, the Archimedes buoyancy force imposed by the fluid on a particle is based on the specific gravity of the fluid (including the solid) at this level, which is a function of the solid concentration. Lastly, there is an increase in the viscous drag on the particle because of the higher apparent viscosity caused by the presence of other particles.

For mathematical purposes, batch sedimentation can be divided into three zones depending upon the position of the upper and lower phase boundaries (6). These are generally called the constant, first, and second falling rate zones as shown in Figure 1. The constant rate zone ends when the upper phase boundary ceases to fall linearly. The end of the constant rate zone is marked when the upward moving fluid, initiated by the first sediment, intersects the upper suspension-supernatant interface. The first falling rate period ends when the upper and

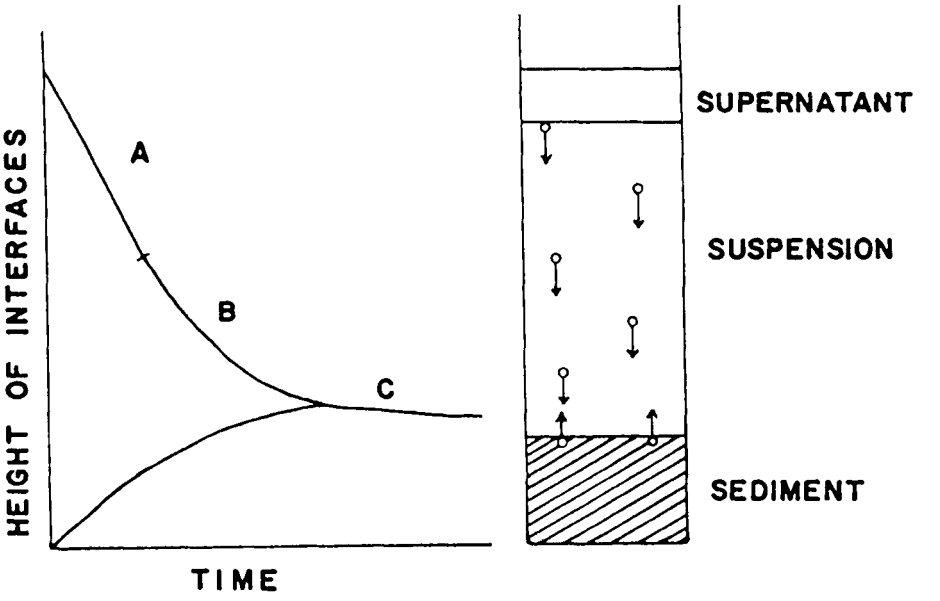

FIGURE 1

Interfaces in sedimentation of a suspension. Key: (A) Constant rate period; (B) First falling rate period; (C) Second falling rate or compression period.

lower phase boundaries merge. At that point, all of the

$$V_S = \frac{d^2(\rho_S - \rho)g}{18\eta} C_H \qquad \text{(Eq. 3)}$$

where C_H is the correction for hindered settling.

As the concentration of the suspension is increased, the observed settling rate falls below V_o, and at some minimum concentration a fundamental change occurs in the appearance of the sedimenting material. At less than this concentration, the suspension exhibits a general cloudiness with the opacity increasing with increasing depth from the surface, during the greater part of the settling time. At and greater than this concentration, an identifiable suspension-supernatant interface

The rheological property of the suspension contributes to settling rate. The rationale for using rheological measurement is that the sedimentation may be considered as if each individual particle falls in a medium composed of the rest of the suspension. Also, it may be argued that both rheological and settling behavior arise from the hydrodynamic interactions between particle and the liquid medium, and so an appreciation of the interactions in rheology would be worth correlating with settling behavior. Rheological behavior of suspensions, especially those containing roughly more than 20% by volume of solids, is complex (7).

A large number of pharmaceutical products, e.g., suspensions, emulsions, natural and synthetic gum solutions show pseudoplastic behavior. Since pseudoplastic curves are nonlinear, viscosity of a pseudoplastic material can not be expressed by a single value.

The mathematical presentation of pseudoplastic flow has been a problem to rheologists. No theoretical equation has been derived from physical concepts, but an empirical power function has been proposed by Porter and Rao (8) to fit the flow curves produced by pseudoplastic materials. Their expression, in the form of more than one constant, is

$$F^N = \eta'(dV/dX) \qquad \text{(Eq. 4)}$$

where F is shearing stress, dV/dX is velocity gradient per unit area, N is a constant and depends on the nature of the system, and η' is the apparent viscosity. The apparent viscosity is not the coefficient of viscosity and does not have the dimensions of the poise. Unlike Newtonian viscosity, η, and plastic viscosity, U, it is difficult to assign any physical meaning to η'. When the value of N varies between zero and one we have pseudoplastic system. Van Wazer et al (9) reported a linear relation when the logarithm of apparent viscosity was plotted against the logarithm of rate of shear.

As an initial step in developing a more complete understanding of sedimentation in concentrated suspensions, a simplified study under conditions of laminar flow was undertaken. It was desirable to produce spherical particles of uniform size to avoid the use of an additional term, the shape factor. The preliminary attempts by several processes indicated that microcapsules would provide uniform spheres. Gelatin and a water soluble drug, Sodium sulfamerazine, were chosen to prepare the microcapsules described elsewhere (10). To minimize the interparticle forces as well as hydration and ionization, a non-aqueous system was selected. Silicone fluids were chosen as dispersion fluid because of their inertness, lack of charge, low surface tension, and availability in various viscosities. The hindered settling of these microcapsules at high concentrations was measured. Various factors were related in an empirical equation.

EXPERIMENTAL

A 5 cm diameter and 70 cm long glass water bath for the sedimentation column, WJC, Figure 2, was prepared. Two 69 cm long pyrex glass tubes with a diameter of 2.22 cm and 2.62 cm were used as sedimentation column, SC. Water was circulated through water bath at 25°C. A fluorescent table lamp, TL, was fixed behind the sedimentation column to enable easy visualization of the suspension supernatant interface. Each column was calibrated at 150 ml and etched.

Approximately 100 ml of silicone fluid of known viscosity at 25±1°C was placed in the sedimentation column. Microcapsules of known size and weight were added to the column and allowed to settle in the fluid. A sufficient amount of the silicone fluid was added to the column until the level of the suspension reached to 150 ml mark. The sedimentation column was held

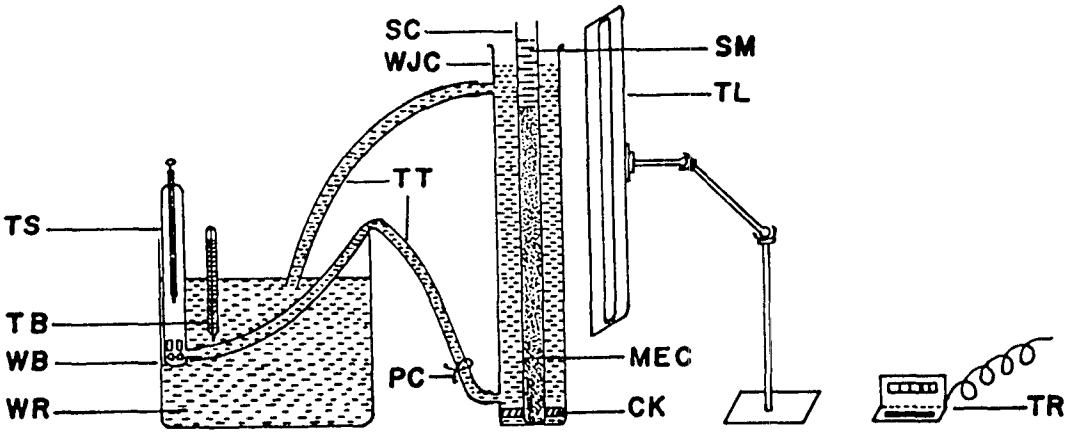

FIGURE 2

Apparatus for sedimentation rate measurements. Key: CK = Cork, MEC = Microcapsules, PC = Pinch cock, SC = Sedimentation column, SM = Suspending medium, TB = Thermometer, TL = Fluorescent table lamp, TR = Timer, TS = Thermostat, TT = Tygon tubing, WB = Water bath, WJC = Water bath for sedimentation column, WR = Water.

between the palms of two hands and the suspension was mixed for 5 minutes by inverting the column several times. The sedimentation column containing the mixed suspension was immediately put into the water bath of the sedimentation column. After the suspension particles fell to a height of 2 to 6 cm (for approximately 1.5 min) from the suspension surface, one could observe the suspension-supernatant interface clearly. At this point a pencil mark was made against the interface on a paper strip taped on the water bath. Five to six readings of the distance travelled by the suspension-supernatant interface against time interval were taken for each sedimentation run. In this manner each sedimentation measurement was repeated for three to six times depending on the precision of the readings.

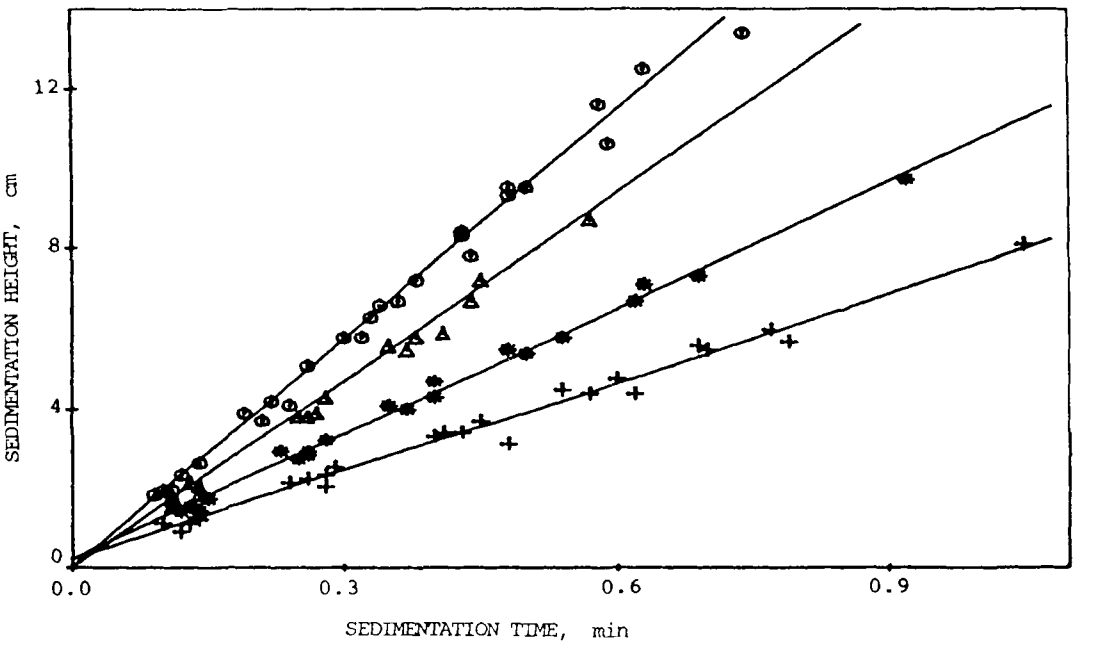

FIGURE 3

Sedimentation height as a function of sedimentation time of 20/30-mesh size microcapsules in 10 cps silicone fluid at 25°C.
Key: ⊙ , suspension concentration = 25%; △ , suspension concentration = 30%; * , suspension concentration = 35%; + , suspension concentration = 40% .

The sedimentation height was plotted against sedimentation time, Figure 3, for each particle size, suspension concentration, and the medium viscosity. The value of the slope determined by linear regression is the sedimentation rate.

A Fisher Surface Tensiometer with a platinum irridium ring was used to measure the surface tension of silicone fluids. The average value of surface tension for all silicone fluids was found to be 22.5 dynes/cm. Silicone fluids have a dielectric constant of 2.5 and show very little change in viscosity with change in temperature.

The Brookfield LVT Viscometer fitted with a # 1 spindle was used to measure the viscosity of silicone fluids used in the sedimentation experiments at various rpm values and at 25°C.

A Stormer Viscometer, having a bob and a cup with central baffle, side vanes, and thermometer holder, was used to determine the viscosity of the suspension, η_s, according to the equation 5

$$\eta_s = K_v(g/RPM) \qquad \text{(Eq. 5)}$$

where K_v is the instrument constant determined for a specific silicone fluid and specific weight, g. Various suspension concen-concentrations used for the study were 25, 30, 35, and 40% w/v. The viscosity of the suspension, η_s, was plotted against the rate of shear, G, for various concentrations in silicone fluids shown in Figure 4.

RESULTS AND DISCUSSION

The curvature of the plots of the viscosity of suspension against rate of shear demonstrate pseudoplastic behavior. At a particular rate of shear, the suspension viscosity increases with an increase in concentration of suspension. These plots were linearized by using the power equation

$$\eta_s{}^N = \eta_k G \qquad \text{(Eq. 6)}$$

where η_s is the suspension viscosity, η_k is the viscosity constant, G is the rate of shear, and N is a constant depending on the system.

The natural logarithm of suspension viscosity, $\ln \eta_s$, was plotted against the natural logarithm of rate of shear, ln G, to yield straight line as shown in Figure 5. The slope (1/N) and

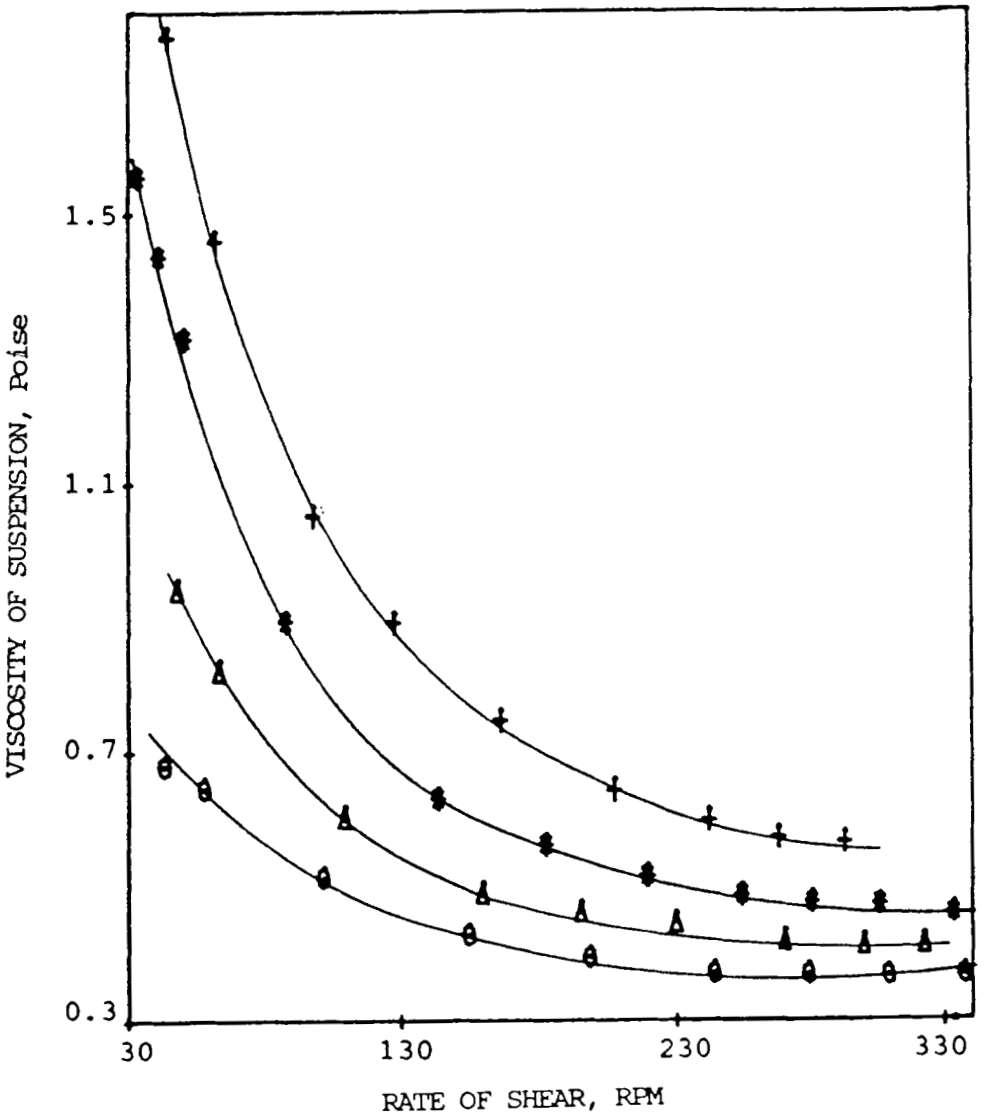

FIGURE 4

Viscosity of suspension of 30/45-mesh size microcapsules as a function of rate of shear in 30 cps silicone fluid at 25°C. Key: ⊙ , suspension concentration = 25%; △ , suspension concentration = 30%; * , suspension concentration = 35%; + , suspension concentration = 40%.

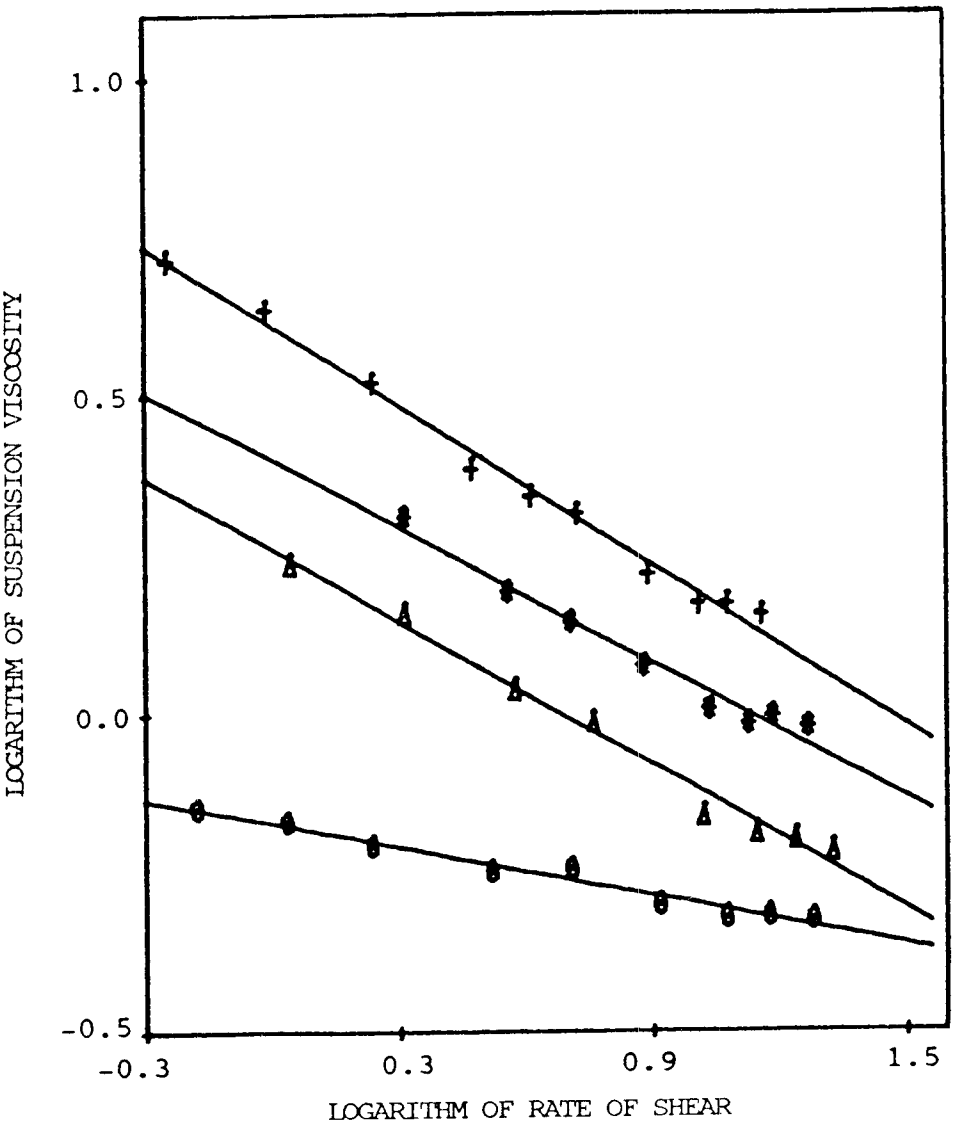

FIGURE 5

Logarithm of suspension viscosity of 20/30-mesh size microcapsules as a function of logarithm of rate of shear in 50 cps silicone fluid at 25°C.
Key: ⊙ , suspension concentration = 25%; △ , suspension concentration = 30%; * , suspension concentration = 35%; + , suspension concentration = 40%.

intercept (1/N ln G) were obtained and the viscosity constant, η_k, was calculated by

$$\eta_k = e^{(\text{intercept/slope})} \qquad \text{(Eq. 7)}$$

The value of viscosity constant changes with the suspension concentration, the diameter of the microcapsule, and the viscosity of the medium.

The present study was confined to large particle sizes, i.e., 725, 478, and 266 microns (20/30-, 30/45-, and 45/80-mesh sizes), at which the effect of Brownian motion is negligible. The microcapsules under study do not show any wetting problem because of lack of charges on their surfaces and the low surface tension of the fluid. The low dielectric constant of silicone fluids assures negligible particle interaction due to double diffuse layer and eliminates the electroviscous force. It fulfills the assumption that the sedimenting particles experience no force other than gravity and viscous drag of the fluid. The examination of microcapsules indicated that they were rigid, discrete, and spherical. Sedimentation rates for 20/30-mesh size particles at 40% concentration in 30 cps silicone fluid were compared in cylindrical columns with diameters of 2.22 and 2.62 cm and found to be insignificantly different from each other. The calculated student t-value was 0.189 and the standard t-value was 2.086 at 95% confidence interval and 20 degrees of freedom. It was assumed that the wall effect can be ignored and it was decided to conduct the sedimentation experiments in a 2.22 cm diameter column.

The effect of particle concentration, medium viscosity, and particle diameter on the sedimentation rate in unflocculated suspensions under conditions of linear flow was determined. The Reynolds number was found to be less than 0.2 for all cases, except for the first case, indicating linear flow conditions. When sedimentation height was plotted against sedimentation

time, it was observed that the linearity of the plot was lost at later times. Such data points were deleted from the sedimentation rate plots. Thus it was assured that the sedimentation rate data used were in the constant rate zone (Figure 1).

When a sedimentation rate plot was examined it was observed that for a medium viscosity and a particle size, as the concentration of the suspension was increased the sedimentation rate decreased indicating greater hinderance to sedimentation. When the viscosity of the medium was increased keeping particle diameter and concentration same, the sedimentation rate decreased due to the greater resistance to particle motion. For the same viscosity and concentration, as the particle size was increased, sedimentation rate increased due to an increase in mass. The Stokes equation (Eq. 2) may be modified to consider variables in concentrated suspension

$$V_S = \frac{d^2(\rho_S - \rho)g}{18\eta} C_H \qquad \text{(Eq. 8)}$$

where C_H is correction for hindered settling. The C_H term may be a function of particle size, suspension concentration, and viscosity constant

$$C_H = f(d, C, \eta_k) \qquad \text{(Eq. 9)}$$

The values of sedimentation rate, V_S, and viscosity constant, η_k, were determined for three sizes of microcapsules, at four different concentrations, and in media of four different viscosities. These data were fitted to the equation

$$V_S = \frac{(\rho_S - \rho)g}{18\eta} d^{\alpha} C^{\beta} \eta_k^{\gamma} \qquad \text{(Eq. 10)}$$

where α, β, and γ are constants. When the sedimentation rate, V_S, was plotted against $[(\rho_S - \rho)g/ 18 \eta]$, a linear relation was

obtained (Figure 6) indicating that there should be a power of one on the bracketted term.

The terms in Eq. 10, for the sedimentation studies were analysed on Minitab Multiple Linear Regression Program operating on a Prime 650 computer at the University of Iowa, Computer Center. The parameters were transformed into natural logarithms:

$$\ln V_s = \ln \frac{(\rho_s - \rho)g}{18\,\eta} + \alpha \ln d + \beta \ln C + \gamma \ln \eta_k \qquad \text{(Eq. 11)}$$

or

$$\ln V_s - \ln \frac{(\rho_s - \rho)g}{18\,\eta} = Y = \alpha \ln d + \beta \ln C + \gamma \ln \eta_k \qquad \text{(Eq. 12)}$$

and the values of the coefficients to best fit the curve was obtained.

A least squares method was used to plot the experimental values of Y against the predicted values of Y in Eq. 12 using the coefficients determined. It was found that the last four experimental values for microcapsules of 0.0266 cm diameter in a medium of 0.9184 poise were significantly different from the regression line and were considered as outliers. The outliers were deleted from the data set, and the statistical test was made. Residual analysis was conducted to investigate the lack of fit of the model, and it was found that there was a slight curvature in the plot of residuals and the fitted values. The curvature disappears if a constant, K, is used in the model. The multiple regression coefficient obtained was 0.985 and 97% of the variation in the predicted values of sedimentation rate could be explained by the model (Figure 7)

$$Y = \alpha \ln d + \beta \ln C + \gamma \ln \eta_k + K \qquad \text{(Eq. 13)}$$

Other statistical results are given in Table 1.

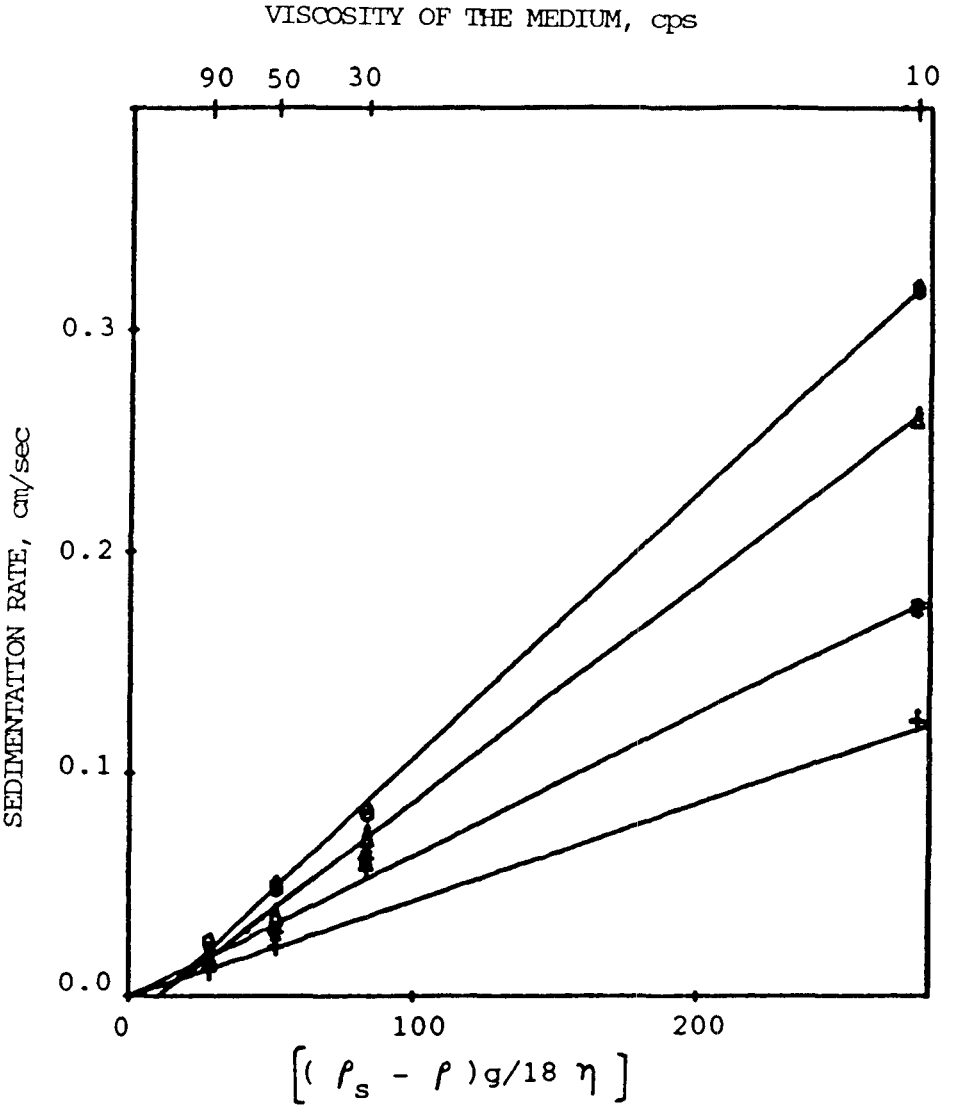

FIGURE 6

Sedimentation rate of 20/30-mesh size microcapsules as a function of $[(\rho^s - \rho)g/18\eta]$ and viscosity of the medium, η at 25°C.
Key: ⊙ , suspension concentration = 25%; △ , suspension concentration = 30%; * , suspension concentration = 35%; + , suspension concentration = 40%.

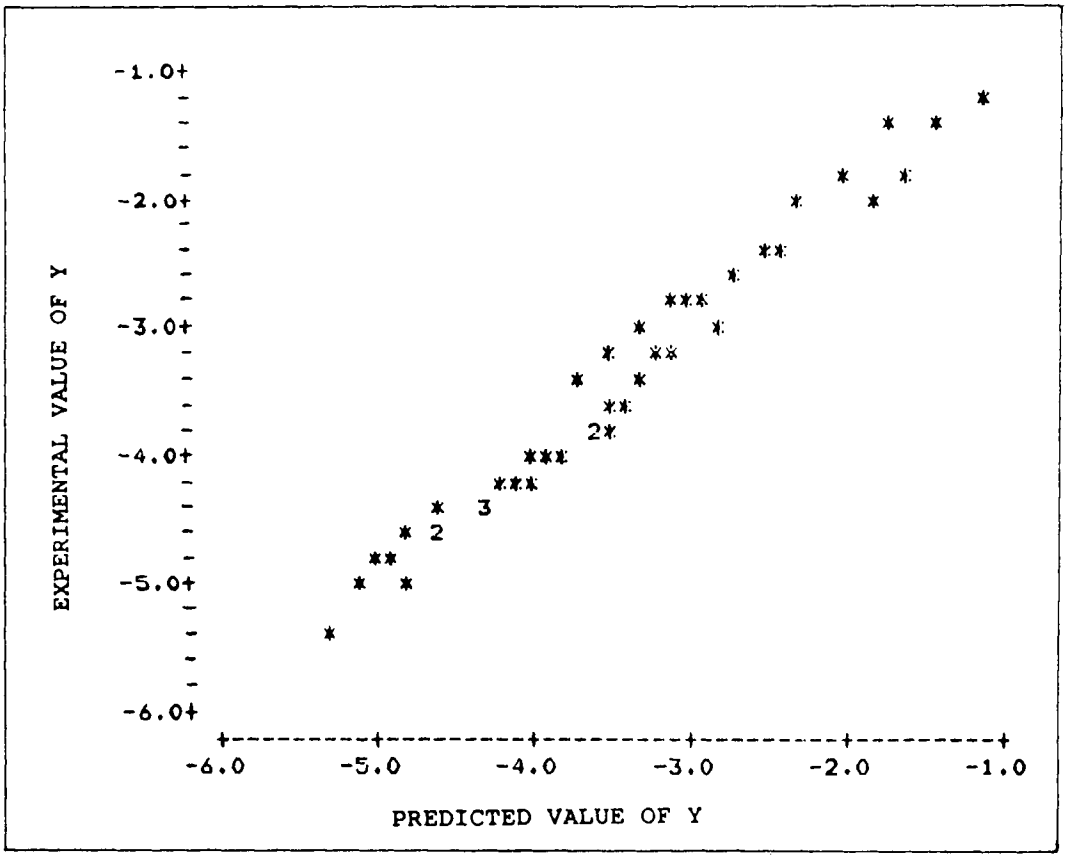

FIGURE 7

Experimental value of Y against predicted value of Y according to the fitted equation for all sizes of microcapsules.

The proposed empirical equation

$$V_s = \frac{(\rho_s - \rho)g}{18\,\eta} d^{1.63} \frac{1}{c^{1.27}} \eta_k^{0.07} e^{-4.31} \qquad \text{(Eq. 14)}$$

was in agreement with the experimental data so far analysed. The unit for the constant, $e^{-4.31}$, is 1/cm.

The above equation predicts the sedimentation rate of an unflocculated suspension at high concentration under the

TABLE 1.

Statistical Analysis of the Empirical Equation:

Parameter	Variable	Coefficient	95% Confidence Limits	Percent Variance Explained
d	α	1.63	0.169	77.13
C	β	-1.27	0.383	14.12
η_K	γ	0.07	0.046	1.53
-	K	-4.31	0.752	-
	Residuals			7.22

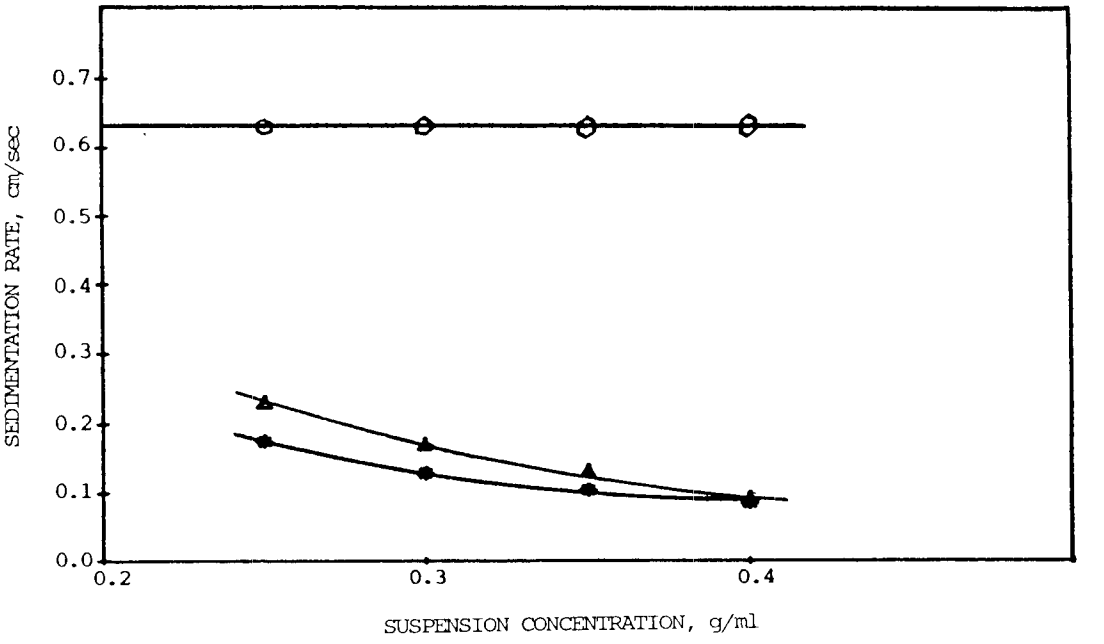

FIGURE 8

Rates of sedimentation predicted by several relationships against suspension concentration for 0.0478 cm. diameter microcapsules in 10 cps medium viscosity.
Key: ◈ , calculated from classical Stokes' equation; ⚠ , experimental values; * , predicted values from the fitted equation.

conditions used in our studies. The exponent of particle diameter is not 2 as in Stokes equation but, it is 1.63 which means that the effective diameter of the particle increases. The effect of concentration is inversely related to sedimentation rate, i.e., as the concentration is increased, the sedimentation rate decreases. The exponent of viscosity constant is quite small which infers that the influence of viscosity of suspension on sedimentation rate is not significant. The constant, $e^{-4.31}$, is due to unidentified variables.

A plot of sedimentation rate, V_s, against suspension concentration, C, for 30/45-mesh size microcapsules in 10 cps silicone fluids is shown in Figure 8, to compare values calculated from the classical Stokes equation, experimental values, and predicted values from the fitted equation. The curve calculated from the classical Stokes equation has a slope of zero, which means that Stokes equation does not predict the effect of concentration on sedimentation rate. The curves obtained from experimental and predicted values are similar with more deviation of predicted values from the experimental values at lower concentration of suspension.

REFERENCES

(1) G. G. Stokes, Mathematical and Physical Papers, 1901.

(2) A. S. Foust, L. A. Wenzel, C. W. Clump, L. Maus, and L.B. Anderson, "Principles of Unit Operations", John Wiley & Sons, New York, 1980, Chapter 22.

(3) T. Allen and M. G. Baudet, Powd. Tech., 18, 131, (1977).

(4) L. Schiller, Handbook of Experimental Physics, Leipzig, 4, 342 (1932).

(5) J. Mizrahi and M. Goldberg, Israel J. of Technology, V7, n5, 385-392 (1969).

(6) Frank M. Tiller, AIChE Journal, V27, n5, 823-829, (September, 1981).

(7) Takeru Higuchi, J. Am. Pharm. Assoc., Sci. Ed., 47, 657, (1958).

(8) A. W. Porter and P. A. M. Rao, Trans. Faraday Soc., 23, 311 (1927).

(9) J. R. Van Wazer, J. W. Lyons, K.Y. Kim, and R.E. Colwell, "Viscosity and Flow Measurements, A Laboratory Handbook of Rheology", Interscience Publishers, N. Y., (1963).

(10) K.C. Dhupar, Ph.D. Thesis, University of Iowa, Iowa City, Iowa 52242, 1982.

(11) A. N. Martin, J. Swarbrick, and A. Cammarata, "Physical Pharmacy", 1970, Chapter 19.